Electromagnetic wave sensors

# Improved Accuracy of Tissue Glucose Measurement Using Low Magnification Optical Coherence Tomography

Tatsuro Miura[1], Akitoshi Seiyama[1], Monte Cassim[1,2], and Junji Seki[3]

[1]*Human Health Sciences, Graduate School of Medicine, Kyoto University, Kyoto-City 606-8507, Japan*
[2]*Akita International University, Akita-City 010-1292, Japan*
[3]*Kansai University, Suita-City 564-8680, Japan*

Manuscript received September 9, 2021; revised October 27, 2021; accepted October 29, 2021. Date of publication November 9, 2021; date of current version November 29, 2021.

Abstract—Optical coherence tomography (OCT) has a comparatively high spatial resolution among tomographic bioimaging techniques and is less affected by changes in physiological conditions such as temperature, blood pressure, and osmolytes in the tissue. OCT detects changes in the refractive index of tissues, which is a function of the tissue glucose concentration (TGC). OCT signal intensity generally decreases with tissue depth, and its slope is expected to show a negative correlation with TGC in the interstitial fluid, reflecting blood glucose concentration. The currently applied OCT system for measuring TGC does not satisfy the accuracy for clinical demand, mainly because of the temporal and spatial variations of living tissues. In this letter, we propose a low magnification OCT (LM-OCT) for noninvasive monitoring of TGC by reducing the spatial resolution and show that LM-OCT significantly improves the accuracy of glucose measurement. The continuous development of LM-OCT in this direction is expected to offer a reliable and noninvasive tool for the clinical monitoring of TGC.

Index Terms—Electromagnetic wave sensors, low-magnification optical coherence tomography (LM-OCT), sensor development, spatiotemporal resolution, tissue glucose concentration (TGC).

## I. INTRODUCTION

The number of patients suffering from diabetes has been increasing year by year and was more than 463 million people worldwide in 2019 [1]. Diabetes causes serious complications, such as retinopathy, nephropathy, and neuropathy. Patients require monitoring and control of blood glucose concentration (BGC) several times per day to avoid disease progression. At present, BGC is monitored in most cases by invasive and uncomfortable methods, both clinically and in daily self-monitoring, because chemical analyses of the invasive methods provide reliable accuracy [2], [3]. In the past two decades, significant efforts have been made to develop noninvasive optical techniques, including near-infrared scattering measurements [4], polarimetry [5], photo-acoustics [6], Raman spectroscopy [7], and optical coherence tomography (OCT) [8]–[16].

Among them, OCT has several advantages for bioimaging because it has high spatial resolution and is less affected by physiological conditions such as temperature, blood pressure, and osmolytes [9], [12]. Therefore, OCT is regarded as a promising method for noninvasive tissue glucose concentration (TGC) in the tissue surface layer [8]–[17]. More recently, subsequent developments in optical techniques for measuring TGC (e.g., polarized-sensitive OCT or Mueller OCT [18] or planar waveguide optical sensors [19]) have been reported; however, their sensitivity and specificity for estimating TGC are still below the clinical demands [2], [3].

It has been reported that temporal and spatial smoothing of OCT signals are effective for improving the precision of TGC measurements [10]. Temporal smoothing reduces measurement variation by averaging the massive data accumulated with multiple scans. Although the development of frequency-domain OCT (FD-OCT) such as swept-source OCT (SS-OCT) and spectral-domain OCT (SD-OCT) has remarkably improved the measurement rate [16], it is still struggling to reach an acceptable level of accuracy in TGC measurements, clinically, and commercially [2], [3]. In contrast, spatial smoothing can reduce data dispersion by smoothing and reducing the inhomogeneity of the tissue structure. Although approaches using 2-D or 3-D scans have been attempted [8], [13], they have also been found to spend considerable measurement time depending on the dimension of the scanning.

In this letter, we propose a new approach for spatial smoothing by applying a low magnification OCT system (LM-OCT) with a wider lateral resolution by using low magnification objective lenses as low as 3×. Therefore, we report the stability and precision of LM-OCT for measuring a wide range of glucose concentration (GC) in *in vitro* phantoms.

## II. EXPERIMENTAL SETUP

### A. Theoretical Background

Light scattering arises from the differences in the refractive indices (RIs) between the interstitial fluid (1.348–1.352) and the intracellular components (1.46–1.48) such as the plasma membrane and the cytosolic component [20]. The RI of interstitial fluid also changes with the GC at a constant rate of $1.515 \times 10^{-6}$ / (mg/dL) [21]. An increase in BGC induces an increase in TGC, resulting in a decrease in light scattering at cellular interfaces due to a reduction in the RI mismatch between the interstitial fluids and cells. Owing to the light extinction within the biological tissue, the OCT signal decreases exponentially

Corresponding author: Akitoshi Seiyama (e-mail: seiyama.akitoshi.7x@kyoto-u.ac.jp).
Associate Editor: Deepak Uttamchandani.
Digital Object Identifier 10.1109/LSENS.2021.3126431

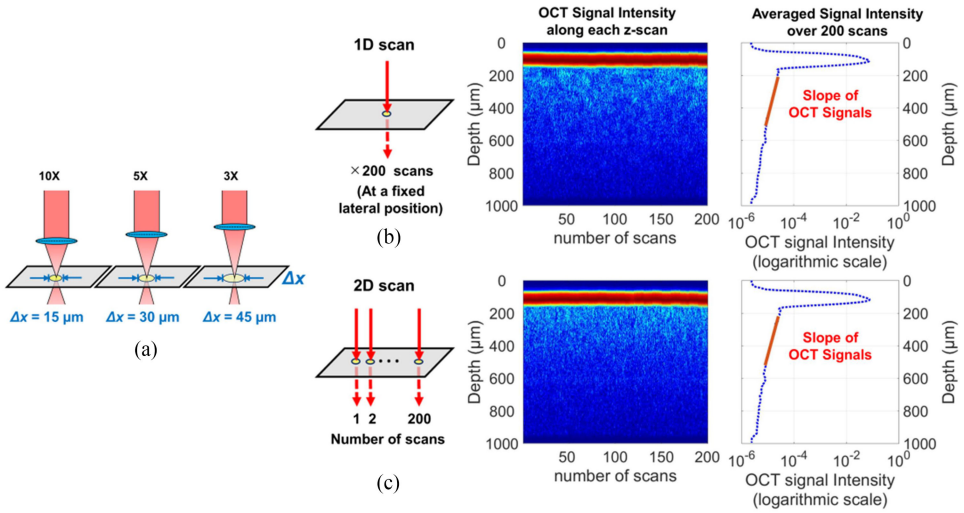


Fig. 1. Measurement areas using LM-OCT system equipped with lenses of 10×, 5×, and 3× (a) and typical examples of the changes in OCT signal intensities as a function of the sample depth obtained by 1-D (b) and 2-D (c) scans with an objective lens of 10×. The values of the logarithm of the signal intensity shown with a pseudocolor in the middle figures are shown in the horizontal axes in the right figures.

as a function of the geometric depth $z$ and is expressed as

$$I\ (z) = I_0\ exp\,(-\mu_t \cdot 2z) \tag{1}$$

where $I_0$ and $I(z)$ are the incident light intensity and light intensity at depth $z$, respectively. $\mu_t$ is the total attenuation coefficient, which is given as $\mu_t = \mu_a + \mu_s$, where $\mu_a$ is the absorption coefficient, and $\mu_s$ is the scattering coefficient. If the light scattering of the sample medium is not isotropic, the light scattering coefficient is practically given as $\mu_s{}' = \mu_s\,(1\text{–}g)$, where $\mu_s{}'$ is the reduced scattering coefficient and $g$ is the anisotropic parameter, and in the near infrared region around 1300 nm, $\mu_s{}' >> \mu_a$ can be assumed for biological tissues, and thus, we obtain the relationship $\mu_t \sim \mu_s{}'$. Accordingly, Eq. (1) can be expressed as

$$\ln I\,(z) = \ln I_0 - 2\mu_s{}' \cdot z\ . \tag{2}$$

Equation (2) indicates that $2\mu_s{}'$ corresponds to the slope of the logarithmic plot of OCT signal intensity versus $z$, which changes with the TGC. In the present study, we used this equation to estimate GC in tissue phantoms.

## B. Tissue Phantom Preparation

For the tissue phantoms for simulating the light scattering property of the biological tissues, we used a suspension of spherical polystyrene particles (0.92 $\mu$m in diameter; Spherotech, Lake Forest, IL, USA) in phosphate buffered saline solution at a fixed concentration. The scattering properties of the particles can be calculated according to the Mie theory, assuming a uniform configuration and size of the particles [22]. Glucose was dissolved in the particle suspension to prepare five GC samples of 0, 5, 10, 15, and 20 g/dL. The estimated scattering property of the sample suspension was set almost equal to that of human skin ($\mu_s$ = 1.0324 mm$^{-1}$, $g$ = 0.81 [23], 2.92 × $10^{-3}$ spheres/$\mu$m$^3$, and pH = 7.1 ± 0.1 at room temperature). The suspension was filled in a transparent quartz cell equipped on the scanning stage, and the measuring light beam was irradiated through the cell wall from the above mentioned direction.

## C. OCT Systems

In the present study, we used a self-made time domain OCT described elsewhere [24]. We configured an LM-OCT system equipped with objective lenses of 10× (LSM02; Thorlabs, Newton, USA), 5× (LSM03; Thorlabs), and 3× (LSM04; Thorlabs) (see Fig. 1(a)).

The lateral resolution $\Delta x$, the waist diameter of the sample beam, is given by

$$\Delta x\ = \frac{4f\lambda}{\pi D} \tag{3}$$

where $f$ is the effective focal length of the objective lens, $\lambda$ is the central wavelength of the light source, and $D$ is the diameter of the incident beam.

The axial resolution of the OCT, $\Delta z$ on the order of the coherence length, is given by

$$\Delta z\ = \frac{2\ln 2}{\pi} \cdot \frac{\lambda^2}{\Delta\lambda_{FWHM}} \tag{4}$$

where $\Delta\lambda_{FWHM}$ is the spectral bandwidth of the light source [11], [16]. The confocal parameter $b$, which is the range in the axial direction where the collimated beam waist is less than the square root of two times the waist on a focal spot, is represented by

$$b\ = \frac{\pi\Delta x^2}{2\lambda}\ . \tag{5}$$

The parameters of the OCT systems equipped with objective lenses of 10×, 5×, and 3× used in this study were $f$ = 18, 36, and 54 mm, respectively, and were $\lambda = 1.3\ \mu$m, $D = 2.0$ mm, and $\Delta\lambda_{FWHM} = 110$ nm overall. The lateral resolutions of the OCT systems were estimated to be 15, 30, and 45 $\mu$m in the air, and the confocal parameters were estimated to be 268, 1073, and 2413 $\mu$m for the objective lenses of 10×, 5×, and 3×, respectively. The axial resolution of the OCT systems was estimated to be 7 $\mu$m in the air.

## D. OCT Measurement and Analysis

Experiments were performed using the LM-OCT systems equipped with lenses of 10×, 5×, and 3× by 1-D and 2-D scans. At a fixed lateral position of the sample beam, a 1-D scan along the $z$ axis (in the

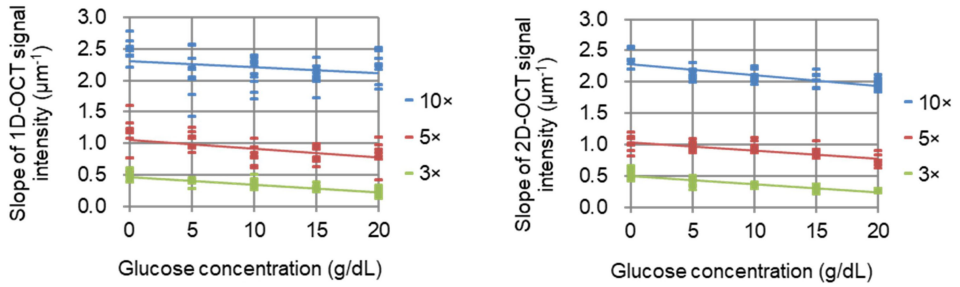


Fig. 2. Slope of OCT signal intensity versus depth plotted against the GC in the phantom. (a) 1-D. (b) 2-D scan measurements. Each line indicates the linear regression.

depth direction of the object) was achieved by scanning the reference mirror by 1 mm. In the 1-D scan, OCT signals were obtained from 200 continuous scans without moving the sample stage. In the 2-D scan, OCT signals were obtained from 200 $z$-scans by moving the sample stage laterally in 10-$\mu$m steps each time the $z$-scan was completed. Both the 1-D and 2-D scan data consisted of 200 $z$-scans. These two types of measurements were repeated 10 times each for sample suspensions with GC of 0, 5, 10, 15, and 20 g/dL. In both the 1-D and 2-D scans, 200 continuous $z$-scans required about 50 s. For each dataset consisting of 200 continuous $z$-scans, the OCT signals were transformed into logarithmic values and were averaged to reduce the speckle noise. The slope of the averaged OCT signals versus depth, which is the attenuation constant, was calculated for the range of the optical path length between 100 and 400 $\mu$m from the sample surface. Ten datasets were measured for each sample with a fixed GC. These processes were repeated for the samples with five different GCs. The slopes of OCT signal intensity versus GCs were analyzed using linear regression.

## III. RESULTS AND DISCUSSIONS

### A. Profile of the OCT Signal Change in the Phantom Medium

Fig. 1 shows a typical example of the changes in the OCT signal intensities obtained by the 1-D (top) and 2-D (bottom) scans with an objective lens of 10×. In the middle figures, the signal intensity along each $z$-scan is shown for one data set obtained with 200 continuous $z$-scans. In Fig. 1(right), the averaged signal intensities over 200 scans are shown. The depth is expressed as the optical path length. In Fig. 1(b) and (c), the sharp peaks observed at a depth of around 100–200 $\mu$m correspond to the reflection from the phantom surface. The OCT signals in the semilogarithmic scale decreased almost linearly as a function of the depth. The slope, i.e., the OCT signal decrement with the depth, corresponds to $-2\mu_s$' from Eq. (2). Similar profiles of the OCT signal change were obtained with objective lenses of 5× and 3×.

### B. Effects of the Magnification of the Objective Lenses on the Slope of the OCT Signals

Fig. 2 shows the changes in the slope of OCT signal intensity versus depth plotted against the GC obtained by 1-D scans (a) and 2-D scans (b). Under the glucose-free condition, the slopes of the OCT signal intensity obtained with objective lenses of 10×, 5×, and 3× were 2.21 ± 0.27 (mean ± SD), 0.92 ± 0.22, and 0.34 ± 0.10 in the 1-D measurement, respectively [see Fig. 2(a)]. Those of the 2-D measurement were 2.11 ± 0.17, 0.91 ± 0.13, and 0.37 ± 0.11, respectively [Fig. 2(b)]. These results indicate that a lower magnification results in smaller slope values probably because of the flattening or reduction of the scattering coefficient.

Table 1. Linear Regression Parameters of the Slope of OCT Signal Intensity Versus Glucose Concentration.

| Scan | Lens | $a/10^{-2}$ | $b$ | $R$ | $W_{95}(a)$ | $\lvert W_{95}(a)/a\rvert$ |
|---|---|---|---|---|---|---|
| 1D | 10× | -1.03 | 2.3 | -0.27 | $1.1 \times 10^{-2}$ | 1.02 |
| | 5× | -1.40 | 1.1 | -0.46 | $7.9 \times 10^{-3}$ | 0.56 |
| | 3× | -1.17 | 0.46 | -0.80 | $2.5 \times 10^{-3}$ | 0.22 |
| 2D | 10× | -1.77 | 2.3 | -0.76 | $4.4\times10^{-3}$ | 0.25 |
| | 5× | -1.32 | 1.0 | -0.72 | $3.7\times10^{-3}$ | 0.28 |
| | 3× | -1.26 | 0.49 | -0.82 | $2.6\times10^{-3}$ | 0.21 |

### C. Effects of Magnification of the Objective Lens on the Accuracy in Estimating the Glucose Concentration

Table 1 shows the regression analysis applied to the data shown in Fig. 2. The slope coefficient of the linear regression ($a$) and the width of the 95% confidence interval for the slope coefficient ($W_{95}$) are listed in Table 1. It is apparent that the ratio $|W_{95}/a|$ is smaller for the 2-D scan mode than for the 1-D scan mode for all the magnification objective lenses. Furthermore, the ratio $|W_{95}/a|$ of the lowest magnification objective lens was the smallest in both modes. These results indicate that spatial smoothing, both by 2-D scanning and by using a lower magnification objective lens, produces additive effects to improve the signal-to-noise ratio of the OCT signals. This effect may be attributed to the reduction in the mesoscopic heterogeneity of the sample. Although the suspension used in this study is considered homogeneous macroscopically, the number of suspended particles within the OCT sampling volume, that is the determinant of the OCT signal intensity, changes largely on the position statistically due to its small size. The number also depends on time due to Brownian motion of the suspended particles. The statistic of the particle number with position (2-D scan) is considered different from that with time (1-D scan). In the present case, a 2-D scan with an objective lens of 3× can offer the most accurate parameters for estimating the GC of the sample.

This effect of using low magnification objective lenses is considered to reduce the mesoscopic heterogeneity of the sample medium. In the evaluation of TGC using OCT, spatial smoothing has been attempted

so far by using 2-D or 3-D scans while maintaining a high lateral resolution [8], [13]. However, these approaches have been found to spend considerable measurement time, depending on the dimension of the scanning. Our proposed LM-OCT has the potential to be an efficient method for improving the accuracy of tissue glucose measurement in addition to temporal and spatial smoothing.

The experiments in this study focused on stability and precision of the regression lines by measuring *in vitro* samples with broad range of GCs. In order to apply this method clinically, it is necessary to improve sensitivity for the clinical level of GCs. The methods to realize this goal contain improvement of statistics by finding an optimum magnification of objective, speeding up the OCT scan by use of FD-OCT, and so on.

Furthermore, it is far simpler than other OCT systems such as polarized-sensitive OCT or Mueller OCT [17], and it is also applicable to other OCT systems. In combination with FD-OCT, such as SS-OCT and SD-OCT, our proposed LM-OCT is expected to considerably shorten the measurement time. It should be noted that the OCT measurements in this study aimed to estimate the GC in the interstitial fluid of the tissue surface layer, which consists of the epidermis, dermis, and subcutaneous tissue. The time lag of GC in the skin surface layer reaching the level in the circulating blood glucose is approximately 0–45 min (average lag time: 8–10 min), depending on the physiological conditions of the subjects [25]. Therefore, this time lag should be considered in *in vivo* applications.

## IV. CONCLUSION

In this letter, we examined the effects of spatial smoothing by lowering the magnification of the objective lens in estimating GC in the tissue phantom suspension using LM-OCT. The results showed that the use of lower magnification objective lenses substantially improved the accuracy of the estimation of GC.

The present results suggest more beneficial effects of using LM-OCT under a multidimensional-mode scan on the glucose estimation by smoothing and reducing the inhomogeneity of the tissue structure and such use of LM-OCT is expected to advance noninvasive glucose measurement for patients with diabetes mellitus.

## ACKNOWLEDGMENT

This work was supported in part by the JSPS KAKENHI under Grant JP19H04459 and in part by the Japan Health Foundation. The authors would like to thank Dr. T. Suzuki (Osaka Prefecture University) and Y. Ooi (Osaka University) for their fruitful discussions.

## REFERENCES

[1] Int. Diabetes Fed. (IDF), IDF Diabetes Atlas 9th Edition, 2019. Accessed: Aug. 25, 2021. [Online]. Available: http://www.diabetesatlas.org/

[2] W. Villena Gonzales, A. T. Mobashsher, and A. Abbosh, "The progress of glucose monitoring—A review of invasive to minimally and non-invasive techniques, devices and sensors," *Sensors*, vol. 19, 2019, Art. no. 800, doi: 10.3390/s19040800.

[3] M. Shokrekhodaei and S. Quinones, "Review of non-invasive glucose sensing techniques: Optical, electrical and breath acetone," *Sensors*, vol. 20, 2020, Art. no. 1251, doi: 10.3390/s20051251.

[4] K. Maruo, M. Tsurugi, M. Tamura, and Y. Ozaki, "In vivo noninvasive measurement of blood glucose by near-infrared diffuse-reflectance spectroscopy," *Appl. Spectrosc.*, vol. 57, no. 10, pp. 1236–1244, 2003, doi: 10.1366/000370203769699090.

[5] R. R. Ansari, S. Böckle, and L. Rovati, "New optical scheme for a polarimetric-based glucose sensor," *J. Biomed. Opt.*, vol. 9, pp. 103–115, 2004, doi: 10.1117/1.1626664.

[6] J. Kottmann, J. M. Rey, J. Luginbühl, E. Reichmann, and M. W. Sigrist, "Glucose sensing in human epidermis using mid-infrared photoacoustic detection," *Biomed. Opt. Exp.*, vol. 3, pp. 667–680, 2012, doi: 10.1364/BOE.3.000667.

[7] O. Lyandres, J. M. Yuen, N. C. Shah, R. P VanDuyne, J. T. Walsh, Jr., and M. R. Glucksberg, "Progress toward an in vivo surface-enhanced raman spectroscopy glucose sensor," *Diabetes Technol. Ther.*, vol. 10, pp. 257–265, 2008, doi: 10.1089/dia.2007.0288.

[8] R. O. Esenaliev, K. V. Larin, and I. V. Larina, "Noninvasive monitoring of glucose concentration with optical coherence tomography," *Opt. Lett.*, vol. 26, pp. 992–994, 2001, doi: 10.1364/OL.26.000992.

[9] K. V. Larin, M. Motamedi, T. V. Ashitkov, and R. O. Esenaliev, "Specificity of noninvasive blood glucose sensing using optical coherence tomography technique: A pilot study," *Phys. Med. Biol.*, vol. 48, pp. 1371–1390, 2003, doi: 10.1088/0031-9155/48/10/310.

[10] A. I. Kholodnykh, I. Y. Petrova, K. V. Larin, M. Motamedi, and R. O. Esenaliev, "Precision of measurement of tissue optical properties with optical coherence tomography," *Appl. Opt.*, vol. 42, pp. 3027–3037, 2003, doi: 10.1364/AO.42.003027.

[11] M. Kinnunen, R. Myllylä, T. Jokela, and S. Vainio, "In vitro studies toward noninvasive glucose monitoring with optical coherence tomography," *Appl. Opt.*, vol. 45, pp. 2251–2260, 2006, doi: 10.1364/AO.45.002251.

[12] V. V. Sapozhnikova, D. Prough, R. V. Kuranov, I. Cicenaite, and R. O. Esenaliev, "Influence of osmolytes on in vivo glucose monitoring using optical coherence tomography," *Exp. Biol. Med.*, vol. 231, pp. 1323–1332, 2006, doi: 10.1177/153537020623100806.

[13] R. V. Kuranov, V. V. Sapozhnikova, D. S. Prough, I. Cicenaite, and R. O. Esenaliev, "In vivo study of glucose-induced changes in skin properties assessed with optical coherence tomography," *Phys. Med. Biol.*, vol. 51, pp. 3885–3900, 2006, doi: 10.1088/0031-9155/51/16/001.

[14] V. V. Sapozhnikova, R. V. Kuranov, I. Cicenaite, R. O. Esenaliev, and D. S. Prough, "Effect on blood glucose monitoring of skin pressure exerted by an optical coherence tomography probe," *J. Biomed. Opt.*, vol. 13, 2008, Art. no. 021112, doi: 10.1117/1.2909671.

[15] M. G. Ghosn, N. Sudheendran, M. Wendt, A. Glasser, V. V. Tuchin, and K. V. Larin, "Monitoring of glucose permeability in monkey skin in vivo using optical coherence tomography," *J. Biophoton.*, vol. 3, pp. 25–33, 2010, doi: 10.1002/jbio.200910075.

[16] M. Wojtkowski, "High-speed optical coherence tomography basics and applications," *Appl. Opt.*, vol. 49, pp. D30–D61, 2010, doi: 10.1364/AO.49.000D30.

[17] Y. T. Lan, Y. P. Kuang, L. P. Zhou, G. Y. Wu, P. C. Gu, and H. K. Wei, "Noninvasive monitoring of blood glucose concentration in diabetic patients with optical coherence tomography," *Laser Phys. Lett.*, vol. 14, no. 6, 2017, Art. no. 035603 , doi: 10.1088/1612-202X/aa58c0.

[18] T. L. Chen, Y. L. Lo, C. C. Liao, and Q. H. Phan, "Noninvasive measurement of glucose concentration on human fingertip by optical coherence tomography," *J. Biomed. Opt.*, vol. 23, 2018, Art. no. 047000, doi: 10.1117/1.JBO.23.4.047001.

[19] A. Dutta and P. P. Sahu, "Optical waveguide sensor as detection element for lab on a chip sensing application," in *Planar Waveguide Optical Sensors*, A. Dutta, B. Deka, P. P. Sahu Cham, Switzerland: Springer, 2016; pp. 151–171. doi: 10.1007/978-3-319-35140-7_6.

[20] V. V. Tuchin, "Optical properties of tissue with strong (multiple) scattering. Chap. 1," in *Tissue Optics: Light Scattering Methods and Instruments for Medical Diagnostics*, 2nd ed. Bellingham, WA, USA: SPIE, 2007, pp. 3–152, doi: 10.1117/3.684093.ch1.

[21] J. S. Maier, S. A. Walker, S. Fantini, M. A. Franceschini, and E. Gratton, "Possible correlation between blood glucose concentration and the reduced scattering coefficient of tissues in the near infrared," *Opt. Lett.*, vol. 19, pp. 2062–2064, 1994, doi: 10.1364/OL.19.002062.

[22] H. C. van de Hulst, *Light Scattering by Small Particle*. Downers Grove, IL, USA: Dover, 1981.

[23] V. M. Kodach, D. J. Faber, J. van Marle, T. G. van Leeuwen, and J. Kalkman, "Determination of the scattering anisotropy with optical coherence tomography," *Opt. Express*, vol. 19, pp. 6131–6140, 2011, doi: 10.1364/OE.19.006131.

[24] Y. Satomura, J. Seki, Y. Ooi, T. Yanagida, and A. Seiyama, "In vivo imaging of the rat cerebral microvessels with optical coherence tomograph," *Clin. Hemorheol. Microcirc.*, vol. 31, pp. 31–40, 2004.

[25] E. Cengiz and W. V. Tamborlane, "A tale of two compartments: Interstitial versus blood glucose monitoring," *Diabetes Technol. Ther.*, vol. 11, pp. S-11–S-16, 2009, doi: 10.1089/dia.2009.0002.